Dyes and Pigments 132 (2016) 185–193

Contents lists available at ScienceDirect

Dyes and Pigments

journal homepage: www.elsevier.com/locate/dyepig

Classical or inverted photovoltaic cells: On the importance of the morphology of the organic layers on their power conversion efficiency

F. Martinez [a], Z. El Jouad [b, h], G. Neculqueo [a], L. Cattin [d], S. Dabos-Seignon [c], L. Pacheco [e, f], E. Lepleux [e, f], P. Predeep [g], J. Manuvel [g], P. Thapppily [g], M. Addou [h], J.C. Bernède [b, *]

[a] Departamento de Ciencia de los Materiales, Facultad de Ciencias Físicas y Matemáticas, Universidad de Chile, Casilla 2777, Santiago, Chile
[b] Université de Nantes, MOLTECH-Anjou, CNRS, UMR 6200, 2 rue de la Houssinière, BP 92208, Nantes, F-44000, France
[c] Université d'Angers, Laboratoire MOLTECH-Anjou UMR-CNRS 6200, 2 Bd Lavoisier, 49045, Angers Cedex, France
[d] Université de Nantes, Institut des Matériaux Jean Rouxel (IMN), CNRS, UMR 6502, 2 rue de la Houssinière, BP 32229, 44322, Nantes Cedex 3, France
[e] CSInstrument, 2 rue de la Terre de Feu, 91940, Les Ulis, France
[f] Scientec, 17 Avenue des Andes, Bâtiment Le cèdre, 91940, Les Ulisd, France
[g] Laboratory for Molecular Photonics and Electronics, Department of Physics, National Institute of Technology, Calicut, 673 601, Kerala, India
[h] Laboratoire Optoélectronique et Physico-chimie des Matériaux, Université Ibn Tofail, Faculté des Sciences BP 133, Kenitra, 14000, Morocco

ARTICLE INFO

Article history:
Received 2 March 2016
Received in revised form
27 April 2016
Accepted 29 April 2016
Available online 30 April 2016

Keywords:
Classical organic solar cells
Inverted organic solar cells
Thin film morphology
Atomic force microscopy
Thiophene derivatives

ABSTRACT

Novel organic thiophene derivatives, (*E*)-Bis-1,2-(5,5″-Dimethyl-(2,2′:3′,2″-terthiophene)vinylene (BSTV) and (*E*)-Bis-1,2-(5,5″-Dimethyl-(2,2′:3′,2″:3′,2‴-tetrathiophene)vinylene (BOTV), with different numbers of thiophene units, have been synthesized. They are introduced into organic photovoltaic cells as electron donor. The both organic photovoltaic cell configurations are probed: classical, *i.e.* with the ITO used as anode, and inverted, *i.e.* with ITO used as cathode. Whatever the cell configuration, the best results are obtained when a double cathode buffer layer Alq_3/Ca is used. Actually, such double cathode buffer layer allows cumulating the advantages of its both constituents. The Alq_3 blocks the excitons and protects the organic electron acceptor from cathode diffusion during its deposition, while the low work function of Ca induces a good band matching at the interface electron acceptor/cathode. On the other hand, it is shown that the organic layer surface morphology is decisive whatever the cell efficiency. While the BSTV layers are homogeneous those of BOTV are not. It follows that, in the case of classical organic photovoltaic cells, leakage currents limits the performances of the cells using BOTV, and better performances are obtained with BSTV. This difficulty is overcome in the case of inverted organic photovoltaic cells. This configuration allows limiting the effect of the inhomogeneities of the donor layer and better efficiencies are obtained with BOTV, which was expected due to its smaller band gap value.

1. Introduction

In the field of renewable energy, the theme concerning organic photovoltaic cells (OPVCs) is one of the most investigated all over the world. Impressive progresses were done during these last ten years [1–4]. However the power conversion efficiency (η) of the OPVCs stays significantly below that of inorganic cells and effort dedicated to the improvement of the OPVCs must be pursued. If organic semiconductor materials exhibit high absorption coefficient, the domain in which they absorb the light is quite narrow, what limits the reachable maximum value by current density (Jsc). Moreover after light absorption and exciton creation it is necessary, not only to separate the carriers of the excitons, but also to collect these carriers through the electrodes. Therefore, among the possible ways to improve the OPVCs efficiency we can try to widen the domain of absorption of the light and we can use new buffer layers at the interfaces electrode/organic material in order to improve the carrier collection. It was shown that it is possible to improve the performance of OPVCs by using small band gap organic materials [3,4]. Moreover, as said above, the insertion of buffer layers at the interface organic materials/electrodes allows improving significantly the device efficiency [5,6]. Power conversion efficiencies over 5% can be achieved with multilayer planar heterojunctions when a cathode buffer layer is present at the interface electron acceptor/cathode [7]. This layer has been called

* Corresponding author.
E-mail address: jean-christian.bernede@univ-nantes.fr (J.C. Bernède).

http://dx.doi.org/10.1016/j.dyepig.2016.04.050
0143-7208/

exciton blocking layer (EBL) because its band gap is substantially larger than those of the organic donor and acceptor, which blocks excitons in the organic layer far from the cathode avoiding any quenching effect at the interface cathode/organic. Moreover, it is well known that improving the band matching at the contact electrode/organic material induces significant improvement of the OPVCs performances [8]. In the case of the cathode it is necessary to use a metal with a small work function. Ca has a very small work function but it is quite unstable and usually Ag or Al is used as cathode, while ITO (indium tin oxide) is used as the anode.

On the other hand, inverted OPVCs (IOPCs) with modified ITO as the transparent cathode and a high W_F metal as the anode were proposed [9–12]. In this architecture the anode is the top electrode. This inverted structure allows improvement of the lifetime of the OPVCs, due to the fact that the C_{60} layer is covered by several layers, which decreases the C_{60} exposure to water vapour and oxygen, moreover, an air stable top electrode can be used [13].

In the present work, we investigate the two possible configurations, classical (OPVC) and inverted (IOPVC) organic photovoltaic cells and we investigate the two possible ways evocated, the broadening of the absorption domain through the use of oligomers of the same family but with different number of units, *i.e.* with different band gaps and the use of double cathode buffer layer, to improve the charge collection.

Both electron donors (ED) pertain to the same oligomer family: the (*E*)-Bis-1,2-(5,5″-Dimethyl-(2,2′:3′,2″-terthiophene)vinylene (BSTV) and the (*E*)-Bis-1,2-(5,5″-Dimethyl-(2,2′:3′,2″:3′,2‴-tetrathiophene)vinylene (BOTV) (Fig. 1) the absorption domain of the former begin at around 540 nm, while that of the latter starts at 660 nm, which corresponds to a smaller band gap. As said above, these two ED were probed in classical and inverted OPVCs. On the other hand, in order to improve the electron collection efficiency, we use a double cathode buffer layer Alq_3/Ca, the cathode being an Al film. We show that, while Alq_3 protect the electron acceptor from Al diffusion, Ca improves the band matching at the interface, which results in a significant improvement of the OPVCs efficiency. About the effect of the decrease of the band gap value on the efficiency of the devices, we show that a significant improvement is obtained only if the organic films morphology is sufficiently homogeneous to prevent high leakage currents.

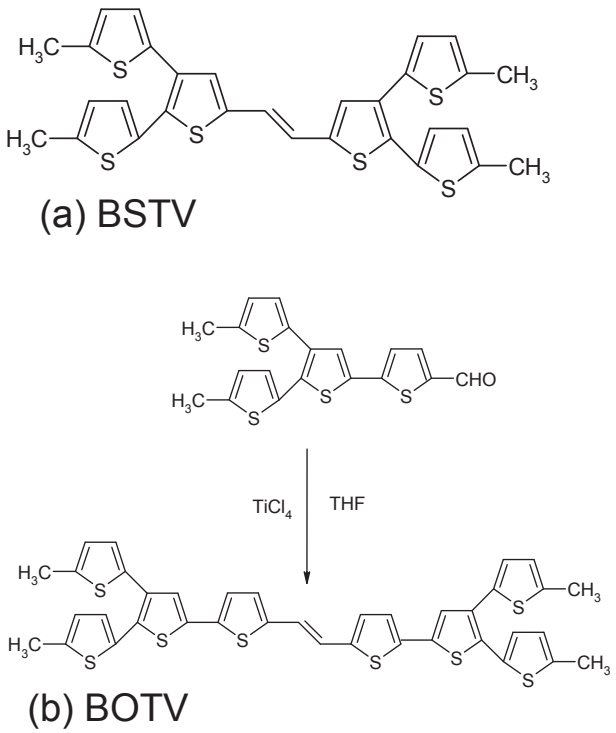

Fig. 1. Scheme of the molecules (a) BSTV, (b) BOTV.

2. Experimental

2.1. Electron donor synthesis

We have already presented the synthesis and characterization of (*E*)-Bis-1,2-(5,5″-Dimethyl-(2,2′:3′,2″-terthiophene)vinylene (BSTV) [13]. We follow a similar process in the case of the (*E*)-Bis-1,2-(5,5″-Dimethyl-(2,2′:3′,2″:3′,2‴-tetrathiophene)vinylene (BOTV) (Fig. 1), but here the "tetrathiophene" is substituted to the terthiophene in such a way that the final product obtained is the (*E*)-Bis-1,2-(5,5″-Dimethyl-(2,2′:3′,2″:3′,2‴-tetrathiophene)vinylene (BOTV).

To a solution of 5,5″-dimethyl-2,2′:3′,2″-terthiophene-5′-carbaldehyde (2 mmol) in anhydrous THF (16 mL) is added titanium tetrachloride (0.7 mL) at −18 °C under Argon atmosphere. The mixture is stirred for one hour at −18 °C. To this solution was added Zinc powder (0.79 g, 12 mmol) in small portions for 10–15 min. The mixture was stirred for 40 min at −18 °C and was then gradually warmed to room temperature and then heated at reflux overnight under argon atmosphere. Then, the mixture was cooled in an ice-water bath and aqueous sodium carbonate solution (50 mL) was added. The organic layer was extracted with chloroform (3 × 50 mL). The combined organic layer were filtered and washed with water until neutral pH. The organic layer was dried over anhydrous $MgSO_4$. The product was purified by column chromatography on silica gel using hexane as the eluent, yielding a red solid (0.55 g; 74% yield), UV–Vis $\lambda_{max} = 460$ nm in $CHCl_3$

^{1}H NMR ($CDCl_3$, 300 MHz) δ (ppm) 7,26 (s, 2H), 7.19–7.00 (m, 3H), 7.01–6.81 (m, 7H), 6.67 (dd, J = 3.4, 1.8 Hz, 4H), 2.55–2.39 (m, 12H).

^{13}C NMR ($CDCl_3$, 75 MHz) δ (ppm) 141.60, 141.57, 140.34, 135.56, 135.07, 134.69, 132.35, 130.76, 127.74, 127.43, 126.80, 126.28, 125.52, 125.37, 124.42, 121.35, 100.01, 15.47, 15.43.

MS (ESI-TOF; $CHCl_3$/MeOH 10:15); *m*/*z* 739.9706 $[M+H]^+$ (calcd. for $C_{38}H_{28}S_8$ 739.9986).

2.2. Characterization technique

The morphology and structure cross section were observed through scanning electron microscopy (SEM) with a JEOL 7600F at the "Centre de microcaractéristion de l'Université de Nantes". The SEM operating voltage was 5 kV. Images were done using secondary electron detector and backscattered electron detector. Optical transmission spectra were recorded by a Carry spectrophotometer. The optical transmission was measured at wavelengths of 1–0.25 μm.

The highest occupied molecular orbital (HOMO) and lowest unoccupied molecular orbital (LUMO) of (*E*)-Bis-1,2-(5,5″-Dimethyl-(2,2′:3′,2″-terthiophene)vinylene (BSTV) and (*E*)-Bis-1,2-(5,5″-Dimethyl-(2,2′:3′,2″:3′,2‴-tetrathiophene)vinylene (BOTV) were evaluated using cyclic voltammetry. A three electrode cell configuration with Pt as the counter electrode is used for this work. Three-electrode configuration allows one electrode to be studied in isolation without complications from the electrochemistry of the other electrodes. The working electrode (here ITO substrate coated with the sample), dipped in an electrolyte solution (Acetonitrile containing 0.1 M tetrabutylammonium tetrafluoroborate-$TBABF_4$), is biased with respect to the reference electrode (Ag/AgCl (3 M NaCl)), which has a known potential. When the bias reaches the

difference between the reference electrode and oxidation potential of the sample, the electrode is oxidized and the current is recorded at the counter electrode. Similarly when the bias overcomes the reduction potential, relative to the reference the electrode is reduced. Here a linear ramping potential starting from zero volt up to a pre-defined limiting value with a scan rate of 50 mV/s and recorded the current. At the optimised limiting potential, the direction of the potential scan is reversed and the current is again recorded. The HOMO and LUMO energy levels are calculated from the following equations:

$$\text{HOMO} = \text{Ionization Potential} = -(E_{ox} + 4.4)\ \text{eV}$$

$$\text{LUMO} = \text{Electron Affinity} = -(E_{red} + 4.4)\ \text{eV}$$

where E_{ox} and E_{red} are onset potentials of oxidation and reduction respectively.

Atomic Force Microscopy (AFM) experiments were performed using the Nano-Observer microscope from C S Instrument. The topographic images were obtained in tapping mode. In addition, this AFM allows resistance and current mapping via the ResiScope mode (from CSInstruments.eu) which is working in contact mode for this experiment. Images were processed using Mountains Map (from Digital Surf).

2.3. Organic photovoltaic cells deposition process and characterization

The ITO coated glass substrates were provided by SOLEMS. After scrubbing with soap, these substrates were rinsed in running deionised water. Then the substrates were dried with an argon flow and loaded into a vacuum chamber (10^{-4} Pa).

In the case of the classical OPVC configuration, the anode buffer layer (ABL) inserted between the ITO anode and the electron donor was the double layer MoO_3/CuI. Actually, we have already shown that this double ABL allows achieving optimized efficiencies [14]. The electron donor used was, as discussed above, a layer of a new thiophene derivative, the BSTV or the BOTV (Fig. 1). The electron acceptor was the fullerene (C_{60}). The cathode was an aluminium film. The CBL was a double-CBL: Alq_3/Ca. Tris-(8-hydroxyquinoline) Aluminium (Alq_3) was chosen because it was shown that it allows growing solar cells with higher lifetime, moreover it has been proven to be a very efficient exciton buffer layer [15]. On the other hand, Ca is known as an efficient electron injecting layer. These chemical products have been provided by CODEX-International (France).

In the case of IOPVCs, about the ABL, it was shown that the use of a 6 nm thick MoO_3 layer allows efficient hole collection to be obtained whatever is the metal of the anode [16]. One of the goals of the present study being to improve the interface cathode/EA, we have used this classical MoO_3/anode hole collecting structure, with an Al metal electrode. In the IOPVCs, ITO when used as the cathode has to be modified using an efficient cathode buffer layer. Since we have shown in a previous publication that the double layer Ca/Alq_3 is efficient as CBL in classical OPVC [17], we have introduced this CBL in the IOPVC used in the present work.

The different layers, MoO_3, CuI, BSTV or BOTV, C_{60}, Alq_3, Ca and Al were deposited in a vacuum of 10^{-4} Pa. The thin film deposition rates and thicknesses were measured *in situ* with a quartz monitor. The deposition rate and the thickness of the MoO_3 layer were 0.02 nm/s and 3 nm respectively [6]. In the case of CuI the deposition rate has a strong influence on the properties of the cells [18]. Actually, it is necessary to deposit this film very slowly to avoid current leakage effect. Therefore the CuI film was deposited at a rate of 0.005 nm/s and its thickness was limited to 1.5 nm. The deposition rate and final thickness were 0.05 nm/s and 40 nm for C_{60}. These thicknesses were chosen after optimization [19]. In the case of OPVCs, we have already shown that the optimum BSTV thickness is 22 nm [17]. The effect of the thickness of the BOTV film on the solar cell performances was studied during the present work. After organic thin film deposition, the aluminium top electrodes were thermally evaporated, without breaking the vacuum, through a mask 2 mm × 12 mm, which gives an effective active area of 0.16 cm^2.

Finally, the structures used were as follow:

-OPVC: glass/ITO(100 nm)/MoO_3(3 nm)/CuI(1.5 nm)/BSTV or BOTV (x nm)/C_{60}(40 nm)/Alq_3(z nm)/Ca (w nm)/Al(120 nm) and
-IOPVC: glass/ITO(100 nm)/Ca (w nm)/Alq_3(z nm)/BSTV or BOTV (x nm)/C_{60}(40 nm)/MoO_3(6 nm)/Al(120 nm).

Electrical characterizations were performed with an automated I-V tester, in the dark and under sun global AM 1.5 simulated solar illumination. Performances of photovoltaic cells were measured using a calibrated solar simulator (Oriel 300W) at 100 mW/cm^2 light intensity adjusted with a PV reference cell (0.5 cm^2 CIGS solar cell, calibrated at NREL, USA). Measurements were performed at an ambient atmosphere. All devices were illuminated through TCO electrodes.

3. Experimental results

Using the OPVC glass/ITO/MoO_3/CuI/BSTV/C_{60}/Alq_3/Ca/Al OPVC we have already shown that the optimum total thickness of the double CBL Alq_3/Ca was 9 nm, while that of BSTV was 22 nm [17]. So, firstly we tried to improve the OPVC performance through the optimisation of the thickness ratio Ca/Alq_3. Then we tested BOTV instead of BSTV and finally the both new ED were probed in IOPVCs.

3.1. Optimization of the double CBL by varying the Ca/Alq_3 thickness ratio

Firstly, we worked on OPVCs using a BSTV layer as ED. The usual thickness of the CBL in planar heterojunction based OPVCs being 9 nm [17], we fix the total thickness of our cathode buffer bi-layer to 9 nm. One can see in Table 1 that the better couple Alq_3/Ca corresponds to 6 nm/3 nm. If we compare the parameters of the OPVCs without Ca in the CBL to those with 3 nm of Ca, it can be seen that if the open circuit voltage Voc is stable, Voc = 0.84 V, the short circuit current Jsc increases significantly, from 3.60 to 5.18 mA/cm^2, while the fill factor decreases slightly, from 50% to 46%. All that results in a

Table 1
Photovoltaic performance data of devices, using BSTV as ED, with different Alq_3/Ca thicknesses, under AM1.5 conditions.

Alq_3 thickness (nm)	Ca thickness (nm)	Voc (V)	Jsc (mA/cm^2)	FF (%)	η (%)	Rs (Ω)	Rsh (Ω)
9	0	0.84	3.60	50	1.47	20	500
7	2	0.83	3.70	50	1.57	20	580
6	3	0.84	5.66	48	2.28	16	650
5	4	0.82	4.16	50	1.71	18	590

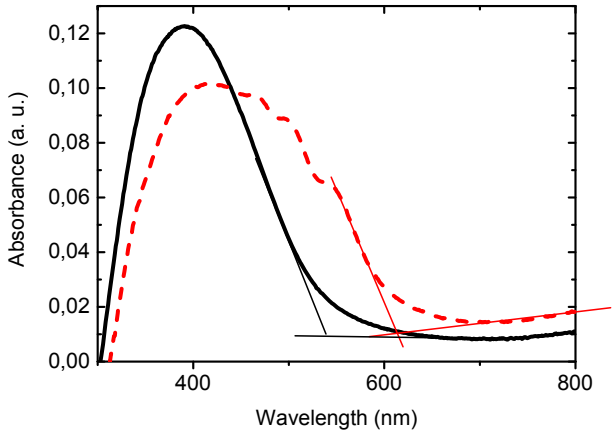

Fig. 2. Absorbance spectra of BSTV (—) and BOTV (– – –) thin films deposited onto ITO.

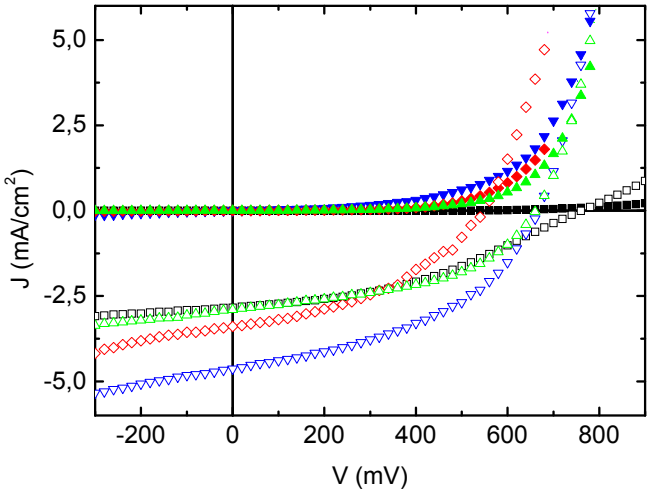

Fig. 3. J-V characteristics of OPVCs with different BOTV thicknesses and cathode bufferlayers: 26 nm (■), 22 nm (▼), 18 nm (◆) all of them with Alq_3/Ca CBL and 22 nm without Ca in the CBL (▲), in the dark (full symbols) and under AM1.5 irradiation (open symbols).

significant efficiency improvement from 1.47% to 2.28% in presence of Ca.

After optimisation of the double CBL, we use it in OPVC probing a new ED, the BOTV.

3.2. OPVCs with BOTV as electron donor

Before testing the BOTV as electron donor in photovoltaic cells, we proceeded to study its absorbance in thin film form. In Fig. 2 we can compare the absorbance range of a BOTV thin film to that of a BSTV thin film. It can be seen that there is a red shift and a broadening of the absorbance spectrum in the case of BOTV. The optical band gaps estimated from these measurements are 2.01 eV for BOTV and 2.28 eV for BSTV.

So, using the already optimized cathode buffer bi-layers, we determined experimentally the optimum thickness of BOTV as electron donor in the OPVCs. It can be seen in Fig. 3 and Table 2 that, as in the case of BSTV, the thickness which allows obtaining the highest efficiency is 22 nm. Also, it can be noted that the effect of Ca is similar with BOTV. As in the case of BSTV, Voc is stable, Jsc increases significantly, while FF decreases slightly. However the maximum efficiencies, 1.36% with Ca in the CBL and 0.9% without Ca, are significantly smaller than those achieved with BSTV. If, here also, Voc is the same with or without Ca, its value is 0.18 V smaller than that obtained with the BSTV. Also FF and Jsc are significantly smaller. All this results in a decrease of the efficiency of the order of 0.5%, whatever the cathode buffer layer is. After the determination of the optimum BOTV thickness, we proceeded to some new depositions to check if the optimum ratio Alq_3/Ca is the same with BOTV as with BSTV. It can be seen in Table 2 that, in the case of CBL bilayer, the efficiency depends only slightly of the Alq_3/Ca ratio. It is probably due to the fact that, as discussed in the paragraph 4, the performance of these cells is mainly limited by the morphology of the BOTV film.

This result is unexpected since, as shown in Fig. 2, the molecule extension BSTV to BOTV induces a red shift and a broadening of the absorption spectrum of the electron donor. This discrepancy will be discussed below after further characterization of the new electron donor layers.

3.3. Additional characterizations

We saw that the use of BOTV instead of BSTV resulting in a significant decrease in OPVC performance. In order to understand the origin of this decrease, we proceeded to study specific properties of the films containing each of the electron donor that can influence the values of the OPVC parameters Voc, Jsc and FF. So we conducted a study by cyclic voltammetry to measure the HOMO and LUMO values of the electron donors and, on the other hand, we studied the morphology of these thin films.

The LUMO and HOMO values calculated form the onset oxidation (reduction) potential are given in Table 3. The potential difference Eg = LUMO-HOMO can be used to estimate the energy gap

Table 3
HOMO, LUMO and band gaps values of the electron donors.

Sample	Eox (V)	HOMO (eV)	Ered (V)	LUMO (eV)	Eg (eV)
HEXAMER	1.25	−5.65	−1.22	−3.18	2.47
OCTAMER	1.19	−5.59	−0.85	−3.55	2.04

Table 2
Photovoltaic performance data of classical OPVCs under AM1.5 conditions with different BOTV thicknesses and with different CBLs.

Alq_3 thickness (nm)	Ca thickness (nm)	Octamer thickness (nm)	Voc (V)	Jsc (mA/cm²)	FF (%)	η (%)	Rs (Ω)	Rsh (Ω)
6	3	18	0.55	3.5	42	0.80	12	350
6	3	22	0.67	4.63	44	1.365	12	430
6	3	24	0.76	2.84	39	0.845	65	550
9	0	22	0.66	2.9	47	0.9	32	430
7.5	1.5	22	0.66	4.37	46	1.34	15	450
4.5	4.5	22	0.64	4.79	43	1.32	12	300

Fig. 4. Surface morphology of a BSTV thin film visualized by SEM.

of the material. It can be seen in Table 3 that the HOMOs values are, in absolute value, 5.65 eV and 5.59 for BSTV and BOTV respectively.

Therefore, the main information deduced from the cyclic voltammetry measurements is that there is a difference of 0.06 eV between the HOMO of BSTV and that of BOTV. As shown in the discussion below, this can be a contribution to the smaller Voc value in the case of BOTV.

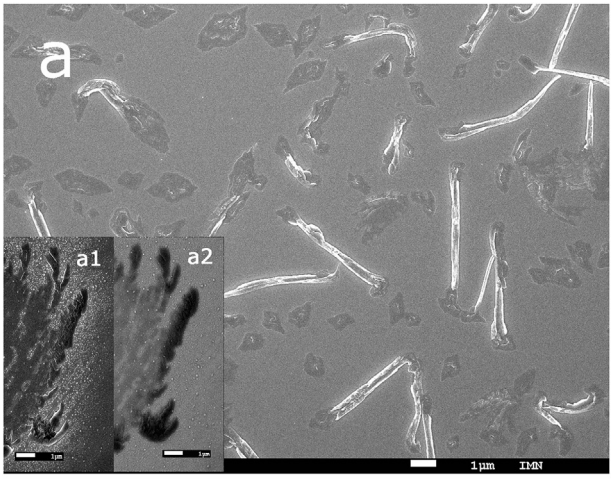

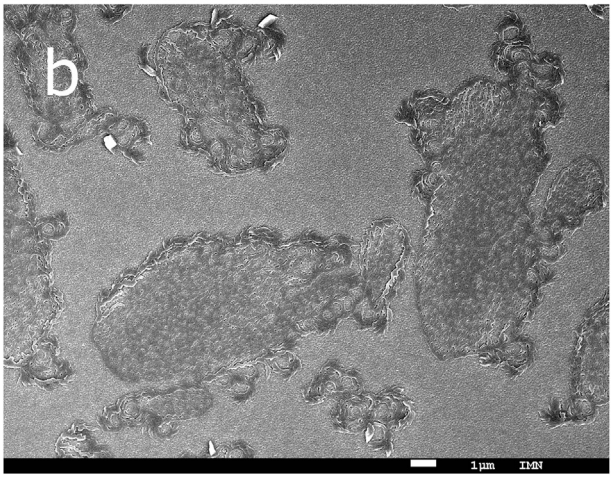

Fig. 5. Surface morphology of a BOTV thin film visualized by SEM (a) in classical and (b) inverted cell configuration. Insert image 5: image of an inhomogeneity in the secondary mode (a1) and backscattering mode (a2).

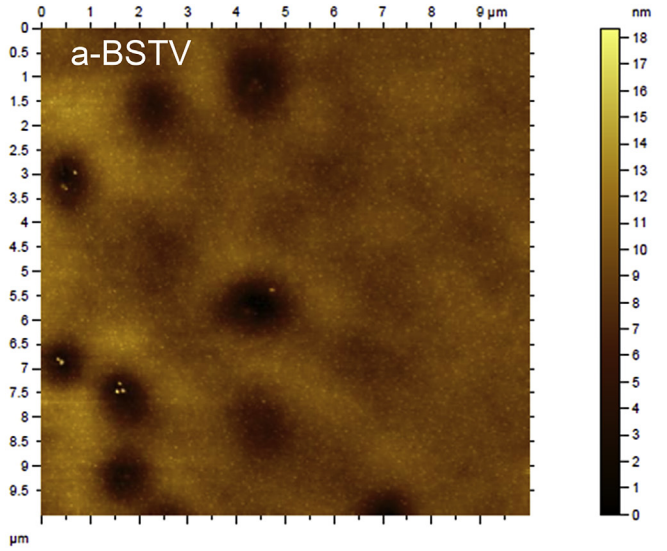

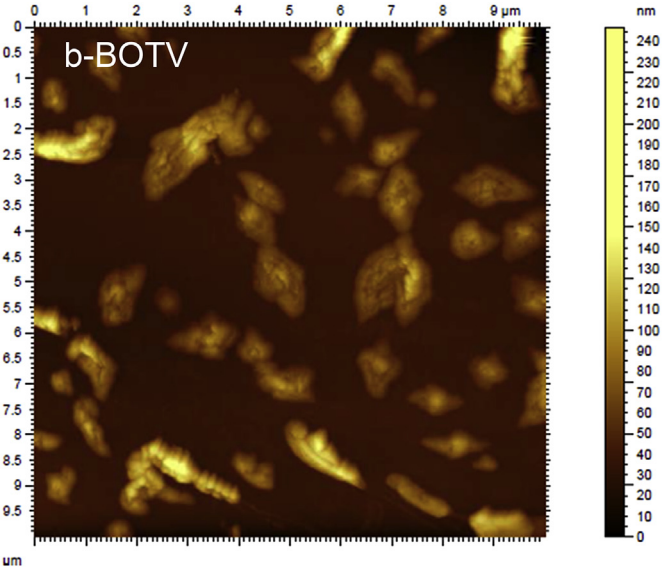

Fig. 6. AFM image of the topography of BSTV (a) and BOTV (b) thin films.

The band gap estimated from these CV measurements can be compared to those estimated from optical measurements. The slight differences, highest band gap values when measured by electrochemistry, are due to the fact that the optical band gaps correspond to the energy needed to form an exciton, while the values deduced from electrochemical measurements correspond to the energies required for an electron to move from the HOMO to the LUMO. This last is the energy required for the formation of an exciton more the energy of the exciton [20].

Another possibility to explain the decrease of the performance of the OPVCs is the morphology of the films [21]. The organic film thickness being very small, any defects in its growth may induce some performance limitation through an increase of the leakage current, so we proceed to a systematic study of the morphology of BSTV and BOTV thin films through SEM and AFM studies.

Figs. 4 and 5 show that the morphology of the films is very different. Whereas BSTV layers are homogeneous those of

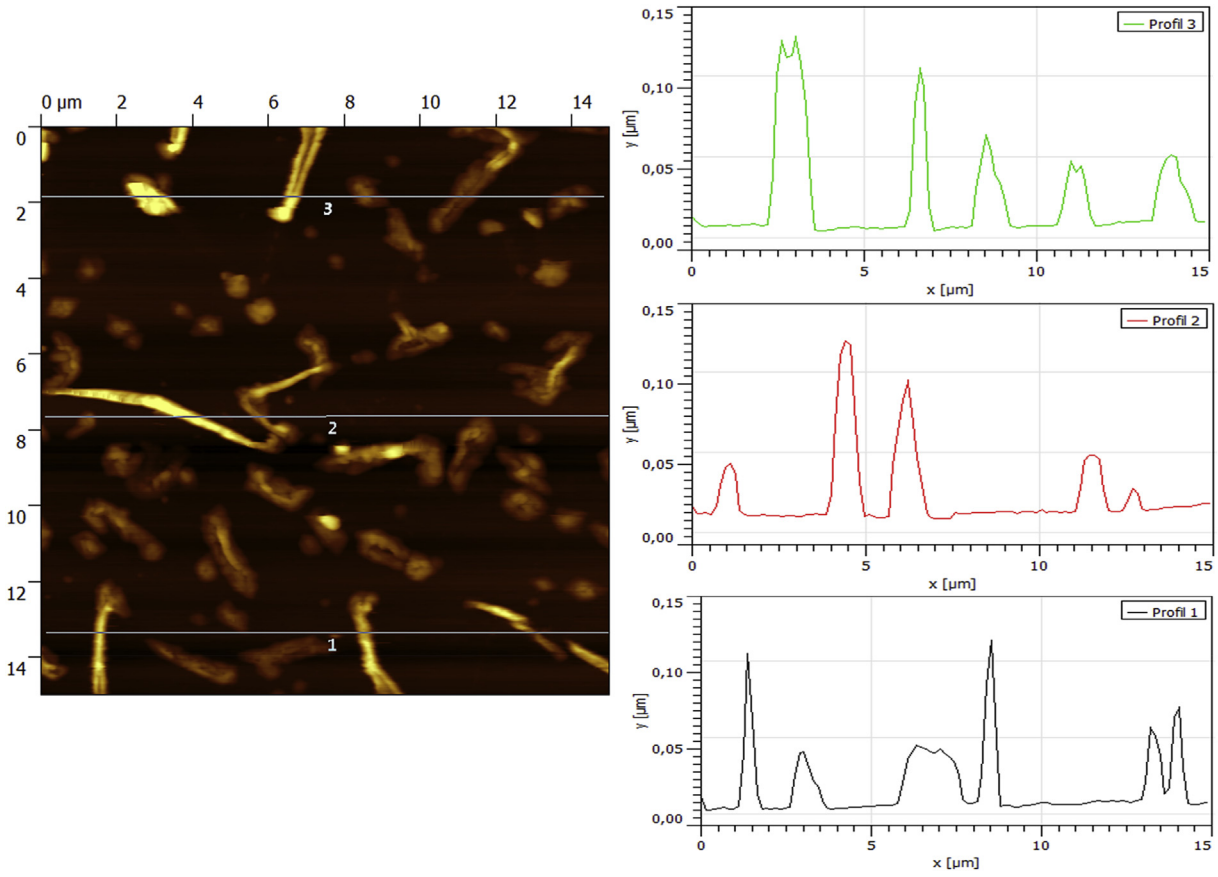

Fig. 7. Extracted profile from BOTV AFM image (15 µm × 15 µm).

BOTV are not, they exhibit a lot of features randomly distributed all over on the surface of the film. In order to check if the inhomogeneities consist of the same atoms as the rest of the layer we performed SEM images for the same area in the secondary and in the backscattering modes. It is known that, in the backscattering mode, the images issued from light atoms are darker, whereas that issued from heavier atoms are brighter. It can be seen in the inset of Fig. 5 that the image corresponding to the backscattering mode (Fig. 5a2) reproduces that of Fig. 5a1, without any colour contrast, the darker zone visible in both images being due to thicker zones, which means that the composition of the film is homogeneous.

The AFM studies (Fig. 6) confirm the surface morphology of the organic films observed by SEM. The roughness parameters allow the quality of the films to be highlighted, thus explaining the obtained performances of the OPVC: while the surface of the BSTV films is rather smooth with a root mean square RMS = 1.54 nm, that of the BOTV films is inhomogeneous with a high value of the RMS, 20.2 nm, within a scan size of 10 µm × 10 µm. Various profiles extracted from the AFM images (Fig. 7) enable to estimate the size of the inhomogeneities observed in the BOTV films. One can notice large clusters with elongate shape whose size exceeds several tens nm. In order to check the possible influence of these inhomogeneities on the current existing in the diode, we proceeded to conductance measurements using the Resiscope mode (from CSInstruments.eu). From this mapping given in Fig. 8, we can notice that the inhomogeneities observed in the topographic image of BOTV (Fig. 8a) correspond to areas of high leakage currents (Fig. 8b). In order to try to minimize this difficulty, we have probed the reverse configuration by growing IOPVC.

3.4. IOPVCs with BSTV and BOTV as electron donor

Using the already optimized Alq_3/Ca cathode buffer bi-layers and MoO_3 ABL, in the IOPVCs, glass/ITO(100 nm)/Ca (3 nm)/Alq_3(6 nm)/BSTV or BOTV (x nm)/C_{60}(40 nm)/MoO_3(3 nm)/Al(120 nm), we have determined experimentally the optimum thickness of BSTV and BOTV. It can be seen in Table 4 and in Fig. 11 that, in the case of BSTV, the highest efficiency is obtained for 22 nm with, Open circuit voltage Voc = 0.65 V, Short circuit current Jsc = 5.27 mA:cm^2, Fill Factor FF = 58% and efficiency η = 1.99%, while in the case of BOTV it is obtained for 26 nm with Voc = 0.57 V, Jsc = 6.88 mA:cm^2, FF = 54% and η = 2.12%. It must be noted that the performances of the IOPVCs are not too different to that obtained with classical OPVC. More important, it can be seen that, as expected, here, the power conversion efficiency of IOPVC using BOTV as ED is higher than that using BSTV.

Fig. 10 shows that, in the case of BOTV the dark current of the IOPVC is far smaller than that measured in the case of OPVC, even if it stays higher than that measured with BSTV, whatever the cell configuration is. Therefore it can be said that the inverted cell configuration allows to decrease the leakage current, which justifies the better efficiency obtained with BOTV in this configuration. The AFM study has shown that the elongated structures visible in the SEM image of Fig. 5a, correspond to areas of high leakage currents (Fig. 8) and we can see in Fig. 5b, that, even if the BOTV film is still not very homogeneous, these elongate structures have disappeared, which justifies the decrease of the leakage current. However, as shown in Fig. 5b, the BOTV film deposited onto C_{60} is still quite inhomogeneous whence the maintenance of some leakage current.

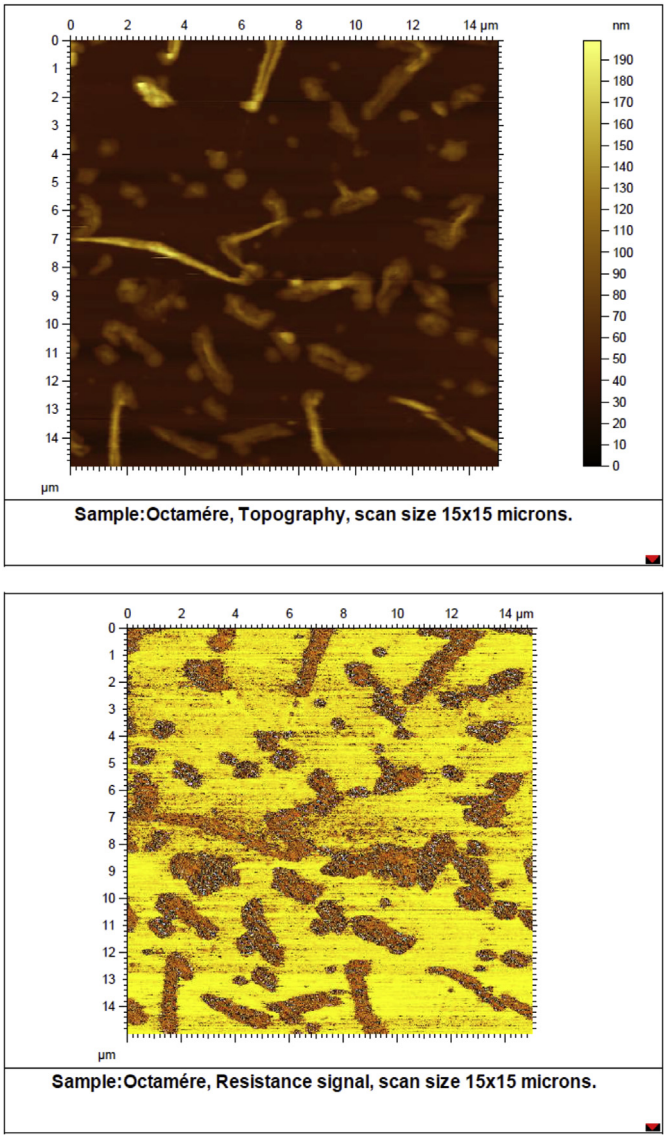

Fig. 8. AFM image of the topography and the conductance of an BOTV thin film.

4. Discussion

We have seen that, using an improved CBL works very well whatever the electron donor is (Tables 1 and 2). These results can be discussed on the basis of the dual function of Alq_3 and Ca. While Alq_3 behaves as an EBL, Ca reduces the electron injection barrier, due to its small work function (2.9 eV). Usually, in the case of classical EBL, the enhancement of the performance of the OPVCs is attributed to several effects such as blocking of the exciton, prevention of metal atom diffusion into the organic electron acceptor during the deposition of the cathode and it can also behave as optical spacer [21,22]. Due to small work function of Ca it is expected to improve the band matching at the interface electron acceptor/cathode.

The interest of the double cathode buffer layer is that it allows cumulating the advantages of each constituent. The Alq_3 EBL blocks the excitons and protects the organic electron acceptor from cathode diffusion during its deposition. A thickness of 6 nm appears sufficient. On the other hand, we have seen that, in small molecule OPVCs, due to the small thickness of the active layer it is necessary to use a reflecting cathode to improve the light absorption. So, if Ca allows a good band matching with a decrease of the series resistance, the low reflectivity of thick Ca films results in lower short circuit current density when its thickness exceeds a certain threshold (Table 1) [23]. Therefore the presence of the EBL allows the use of a very thin Ca film, which prevents these disagreements. Actually, the thin layer of Alq_3 permits all the improvement expected from a classical organic EBL, while the low work function of the ultrathin Ca layer induces high electron collection efficiency, without diminishing the cathode reflectivity.

In the case of OPVC, it must be noted that the BOTV as ED gives an efficiency smaller than that obtained with the BSTV. We saw that the origin of this discrepancy is mainly due to the difference in Voc.

Such behaviour can be due to different origins. Firstly it is now well admitted that the Voc value is such as [22]:

$$Voc = (1/e)\,(LUMO_{EA} - HOMO_{ED}) - a, \quad (1)$$

e being the elementary charge.

Where $LUMO_{EA}$ is the lowest unoccupied molecular orbital of the electron acceptor while $HOMO_{ED}$ is the highest occupied molecular orbital of the electron donor and “a” is an empirical factor, its value depends on the J-V curve of the OPVC. Most OPVCs never reach the maximum theoretical value due to energy loss attributed to charge carrier recombination at the interface [24]. Nevertheless, a difference in the HOMO value of the electron donors may justify a different value in Voc when these electron donors are used with the same electron acceptor.

The relative position of the HOMO-LUMO levels deduced from the cyclic voltammetry measurements is represented in Fig. 9, the HOMO value difference of the two electron donors, which is only 0.06 eV, can partly justify the difference between the measured Voc values (0.17 eV).

Another source of decrease of the OPVC performances is the morphology of the films [3]. The organic film thickness being very small, any defects in its growth may induce some leakage current. As shown in Figs. 4 and 5a the BSTV layers are homogeneous, while that of BOTV are not (Fig. 5b). These results conform to those obtained by AFM.

We estimated the values of the shunt resistance (Rsh) and the

Table 4
Photovoltaic performance data of inverted devices under AM1.5 conditions with different ED (BSEV and BOTV) thicknesses.

Octamer thickness (nm)		Voc (V)	Jsc (mA/cm^2)	FF (%)	η (%)	Rs (Ω)	Rsh (Ω)
BSTV	20	0.61	4.17	57	1.45	10	900
	22	0.65	5.27	58	1.99	10	850
	24	0.65	5.17	53	1.78	18	1200
BOTV	20	0.54	2.96	55	0.88	16	700
	22	0.57	3.25	54	1.00	16	775
	24	0.56	5.31	54	1.60	15	775
	26	0.57	6.88	54	2.12	15	800
	28	0.57	4.81	50	1.48	18	900

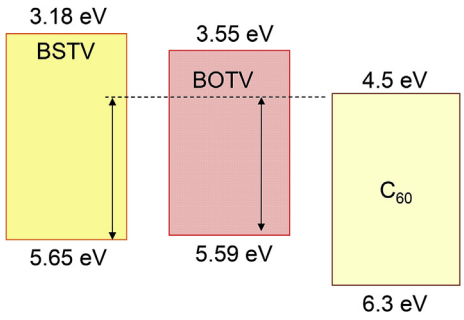

Fig. 9. Energy diagram of materials HOMO and LUMO values of the organic donors and acceptor.

series resistance (Rs), in order to assess the effect of the difference in the film morphology on the values of Rsh and Rs. The slopes at the short circuit point and at the open circuit voltage are the inverse values of Rsh and Rs of the equivalent circuit scheme of a solar cell respectively. The obtained values are reported in Tables 1, 2 and 4. In the case of BOTV, it can be seen that, for the best OPVCs, if Rs is of the same order of magnitude whatever the structure of the cell (OPVC or IOPVC), the values of Rsh are significantly different, the smallest Rsh value being obtained with the classical OPVC configuration, i.e. with the films which are the least homogeneous.

The dark currents as a function of the applied voltage for the optimum OPVCs are reported in Fig. 10. The leakage current in the case of BSTV is negligible until the junction approaches the breakdown conditions. In contrast, in the case of BOTV, the leakage current is significant, which results in a decrease of Voc and FF when the OPVC is submitted to illumination. This can contribute to the better efficiency achieved with the BSTV. This hypothesis is corroborated by the dependence with the ED, of the value of the empirical factor "a" in equation (1). In the case of BSTV: Voc = 0.84 V and therefore, a = 0.31 V. In the case of BOTV, for the best cell, Voc = 0.67 V and a = 0.42 V and for the higher Voc value measured Voc = 0.76 V and a = 0.33 V.

Usually, it is well accepted that a ≈0.3 V. It means that the expected value is obtained for BSTV, but for BOTV it is quite large, mainly in the case of the best cell.

It can be noted Table 1 that Voc does not vary much for BSTV, while it varies quite a lot in the case of BOTV (Table 2), which induces the variation of "a". For thick BOTV film, the leakage current

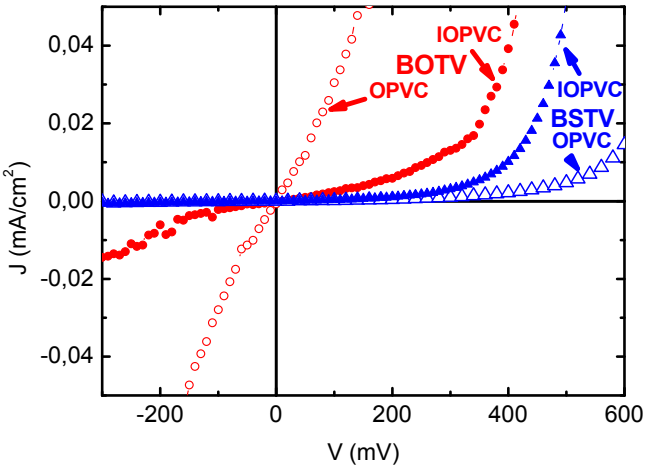

Fig. 10. Dark J-V characteristics of OPVCs (open symbols) and IOPVCs (full symbols) with BOTV (●) and BSTV (▲) as electron donor.

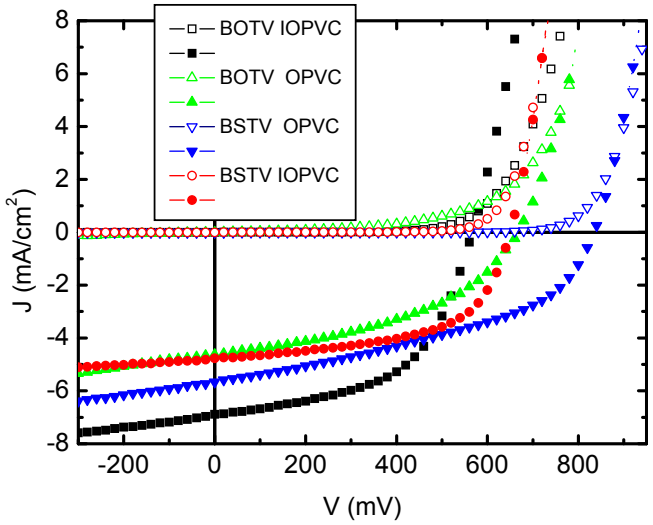

Fig. 11. J-V characteristics of cells with BSTV [(▼-OPVC) (●-IOPVC) and BOTV [(▲-OPVC) (■-IOPVC)], as ED, in the dark (full symbols) and under AM1.5 irradiation (open symbols).

is smaller, Voc is higher and the value of "a" nearly corresponds to the expected value. However, the film is too thick for a good photovoltaic effect and Jsc is small. For thinner BOTV film, "a" increases, so if Jsc is better, Voc decreases. All that confirms the importance of the homogeneity of the organic film on the OPVCs performances.

This negative effect is limited in the case of IOPVCs. In the case of IOPVC, a homogeneous layer of 40 nm thick C_{60}, is deposited onto the cathode before BOTV deposition. This continuous organic film prevents the formation of leakage paths, even if, the BOTV being less homogeneous than BSTV (Fig. 5b), the dark current for the IOPVCs with BOTV is still higher than that obtained with BSTV (Fig. 10). This protective effect of C_{60} in IOPVCs and the disappearance of the elongated structures in the BOTV films allow achieving the expected result, that is to say, a highest efficiency obtained with the ED with the greater number of units, *i.e.* with smaller band gap and wider absorption range.

5. Conclusion

Two electron donors were probed in planar OPVCs, Both electron donors pertain to the same oligomer family: the (*E*)-Bis-1,2-(5,5″-Dimethyl-(2,2′:3′,2″-terthiophene)vinylene (BSTV) and the (*E*)-Bis-1,2-(5,5″-Dimethyl-(2,2′:3′,2″:3′,2‴-tetrathiophene)vinylene (BOTV). After studying the optical properties of these new ED, we show that the integration of the CBL bi-layer, Alq_3/Ca into the OPVCs increases Jsc, which results in a significant improvement of the OPVCs efficiency, whatever the ED is. Unexpectedly, in the case of classical OPVCs, the oligomer with the broader band gap, the BSTV, allows the highest efficiency to be achieved. This fact is attributed to the highest absolute value of the HOMO of BSTV and to the quite poor homogeneity of the films of BOTV. We proceeded to a systematic study of the surface of the new electron donors, BSTV and BOTV, through SEM and AFM and we show that the homogeneity of the surface of the BSTV layer is far higher than that of BOTV. The consequence is that leakage currents are present in BOTV based cells, while they are not in cells using BSTV, which allows this last electron donor to exhibit higher Voc and therefore better efficiencies. In order to prevent this disagreement, we probe IOPVCs, because the presence of the C_{60} layer before the deposition of the ED could prevent the presence of high leakage paths. Using

this cell configuration, the best results are obtained with the oligomer with the smaller band gap value, *i.e.* BOTV.

Acknowledgements

This work was financially supported by the Academy Hassan II (Morocco).

References

[1] Bernède JC. Organic photovoltaic cells: history, principle and techniques. J Chil Chem Soc 2008;53:1549–64.
[2] Kumar P, Chand S. Recent progress and future aspects of organic solar cells. Prog Photovolt Res Appl 2012;20:377–415.
[3] Choi HC, Ko S-J, Kim T, Morin P-O, Walker B, Lee BH, et al. Small-bandgap polymer solar cells with unprecedented short-circuit current density and high fill factor. Adv Mater 2015;27:3318–24.
[4] Hu H, Jiang K, Yang G, Liu J, Li Z, Lin H, et al. Terthiophene-based D–A polymer with an asymmetric arrangement of alkyl chains that enables efficient polymer solar cells. J Am Chem Soc 2015;137:14149–57.
[5] Cattin L, Tougaard S, Stephant N, Morsli S, Bernède JC. On the ultrathin gold film used as buffer layer at the transparent conductive anode/organic electron donor interface. Gold Bull 2011;44:199–205.
[6] Bernède JC, Cattin L, Morsli M. About MoO_3 as buffer layer in organic optoelectronic devices. Technol Lett 2014;1(2):5–17.
[7] Peumans P, Bulovic V, Forrest SR. Efficient photon harvesting at high optical intensities in ultrathin organic double-heterostructure photovoltaic diodes. Appl Phys Lett 2000;79:2650–2.
[8] Godoy A, Cattin L, Toumi L, Diaz FR, del Valle MA, Soto GM, et al. Effects of the buffer layer inserted between the transparent conductive oxide anode and the organic electron donor. Sol Energy Mater Sol Cells 2010;94:648–54.
[9] Zhang F, Xu X, Tang W, Zhang J, Zhuo Z, Wang Jian, et al. Recent development of the inverted configuration organic solar cells. Sol Energy Mater Sol Cells 2011;95:1785–99.
[10] Jiang CY, Sun XW, Zhao DW, Kyaw AKK, Li YN. Low work function metal modified ITO as cathode for inverted polymer solar cells. Sol Energy Mater Sol Cells 2010;94:1618–21.
[11] Zilberberg K, Trost S, Meyer J, Kahn A, Behrendt A, Lützenkirchen-Hecht D, et al. Inverted organic solar cells with sol–gel processed high work-function vanadium oxide hole-extraction layers. Adv Funct Mater 2011;21:4776–83.
[12] Hösel M, Sondergaard RR, Jorgensen M, Krebs FC. Energy Technol 2013;1:102–7.
[13] Hao X, Wang S, Fu W, Sakuri T, Masuda S, Akimoto K. Novel cathode buffer layer of Ag-doped bathocuproine for small molecule organic solar cell with inverted structure. Org Electron 2014;15:1773–9.
[14] Bernède JC, Cattin L, Makha M, Jeux V, Leriche P, Roncali J, et al. MoO3/CuI hybrid buffer layer for the optimization of organic solar cells based on a donor–acceptor triphenylamine. Sol Energy Mater Sol Cells 2013;110:107–14.
[15] Lare Y, Kouskoussa B, Benchouk K, Ouro Djobo S, Cattin L, Diaz FR, et al. Influence of the exciton blocking layer on the stability of layered organic solar cells. J Phys Chem Solids 2011;72:97–103.
[16] Sun F-Z, Shi A-L, Xu Z-Q, Wei H-X, Li Y-Q, Lee S-T, et al. Efficient inverted polymer solar cells with thermal-evaporated and solution-processed small molecular electron extraction layer. Appl Phys Lett 2013;102:133303.
[17] Martinez Francisco, Neculqueo Gloria, Christian Bernède Jean, Cattin Linda, Makha Mohammed. Influence of the presence of Ca in the cathode buffer layer on the performance and stability of organic photovoltaic cells using a branched sexithienylenevinylene oligomer as electron donor. Phys Status Solidi A 2015;212:1767–73.
[18] Makha M, Cattin L, Dabos-Seignon S, Arca E, Velez J, Stephant N, et al. Study of CuI thin films properties for application as anode buffer layer in organic solar cells. Indian J Pure Appl Phys 2013;51:569–82.
[19] Berredjem Y, Karst N, Cattin L, Lkhdar-Toumi A, Godoy A, Soto G, et al. Plastic photovoltaic cells encapsulation, effect on the open circuit voltage. Dyes Pigments 2008;78:148–56.
[20] Gregg BA. The photoconversion mechanism of excitonic solar cells. MRS Bull 2005 Juanuary;30:20–2.
[21] Song QL, Li FY, Yang H, Wu HR, Wang XZ, Zhou W, et al. Small-molecule organic solar cells with improved stability. Chem Phys Lett 2005;416:42–6.
[22] Vogel M, Doka S, Breyer Ch, Lux-Steiner M Ch, Fostiropoulos K. On the function of a bathocuproine buffer layer in organic photovoltaic cells. Appl Phys Lett 2006;89:163501.
[23] Lin H-W, Kang H-W, Huang Z-Y, Chen C-W, Chen Y-H, Lin L-Y, et al. An effective bilayer cathode buffer for highly efficient small molecule organic solar cells. Org Electron 2012;13:1925–9.
[24] Cnops K, Rand BP, Cheyns D, Heremans P. Enhanced photocurrent and open-circuit voltage in a 3-layer cascade organic solar cell. Appl Phys Lett 2012;101:143301.